Memoirs of the Faculty of Engineering, Nagoya University
Vol. 31 No. 2 (1979) — Research Report —

EFFECT OF STATIC IN-PLANE MAGNETIC FIELD ON TRANSLATION VELOCITY AND MOBILITY OF BUBBLE DOMAINS IN Eu-CaGe AND Sm-CaGe SUBSTITUTED GARNET FILMS

SHIGERU SHIOMI, AKIRA IKAI*, YASUSHI SAWADA,
SATOSHI IWATA, SUSUMU UCHIYAMA and TOSHITAKA FUJII**

Department of Electrical Engineering,

(Received November 10, 1979)

Abstract

The effect of static field applied parallel to the film plane on the translation velocity of magnetic bubbles was investigated by usual bubble translation method. In low damping Eu-films, it was found that the translation velocity V of S=0 bubbles having two vertical Bloch lines (VBL's) increases drastically with increasing in-plane magnetic field H_{ip}, but those of two kinds of S=1 bubbles; unichiral bubble having no VBL and σ bubble having a pair of positive and negative polarity VBL's, hardly do. In high damping Sm-films, on the other hand, it was found that V increases only slightly with H_{ip} even for S=0 bubbles. Although the experimental results on high damping Sm-films seem to be explained rather satisfactorily, those on low damping Eu-films seem not to be explained by the current models satisfactorily but to require further consideration.

1. Introduction

Thus far, a lot of both theoretical and experimental efforts have been made in order to understand the dynamic character of bubble domains and resulted in many remarkable achievements. However, there seems to be much left to study. The effect of an in-plane magnetic field on bubble translation velocity may be one of

*) Present Adress: Matsushita Electric Industrial Co. Ltd.,
**) School of Electrical Engineering and Electronics, Toyohashi University of Technology.

the important problems to be studied physically.

The effects of a static in-plane magnetic field on the domain wall dynamics in magnetic bubble garnet films have been studied experimentally[1,2] and theoretically[3]. It has been found that the bubble translation velocity increases with increasing an in-plane magnetic field.[4] However, any clear explanation on the effect of an in-plane magnetic field on bubble translation velocity has not been available to our knowledge, presumably because the improvement of bubble propagation rate or access time by means of an in-plane magnetic field is hardly applicable to field access memory devices developed currently.

In the present study, we have investigated the effect of an in-plane magnetic field on bubble translation velocity and mobility in Eu- and Sm-CaGe substituted garnet films having low and high damping constant, respectively. Special attentions have been paid to the magnetostatic interaction between an in-plane magnetic field and the magnetizations in the bubble wall, and similar experiments were performed for three kinds of bubbles having different wall configuration, respectively.

2. Experimental Procedure

Bubble translation velocity was measured by the method described by Vella-Coleiro and Tabor.[5] The parallel conductors were 10 μm wide and separated 80 μm center-to-center. Throughout the experiment the measurements were done in the narrow region within $\sim$5 μm from the center line between the parallel conductors, because the bias magnetic field compensation was not employed at all. Therefore, appropriate pulse durations longer than 60 nsec were used according to the bubble translation velocity or the bubble displacement per pulsed gradient field. The rise time of pulsed gradient field was about 1 nsec which was the same as the fall time.

We identified bubble states from the skew or deflection angle of bubble translation with respect to the direction of pulsed gradient field.[6] We also used "*bubble automotion*"[7] to identify further detail wall configurations.

The samples used in the present experiment are an as-grown and an ion-implanted films with the two kinds of compositions; $(YEuYbCa)_3(GeFe)_5O_{12}$ and $(YSmLuCa)_3(GeFe)_5O_{12}$. These four films support nominally 3 μm diameter bubbles. The material parameters of the films are listed in Table I. The film thickness h was determined interferrometrically. The saturation magnetization M_s and material characteristic length $l \equiv (AK_u)^{1/2}/\pi M_s^2$ were obtained from stripe-width and bubble collapse measurements. The uniaxial magnetic anisotropy constant K_u and gyromagnetic ratio γ were calculated from the two resonance fields of ferrimagnetic resonance (FMR) $H_{/\!/}$ and $H_\perp$ when a static magnetic field is applied parallel and perpendicular to the film plane, respectively. In these calculations was ignored the cubic magnetic anisotropy K_1. Gilbert damping constant α was calculated from the differential FMR signal assuming Lorentz type absorption. In low damping Eu-films, the calculated values under this assumption agree quite well with the values calculated from the half-line-width obtained by the graphical integration of the differential FMR signal. In high damping Sm-films, however, the differential FMR signal is not symmetric with respect to the resonance field $H_{/\!/}$ or $H_\perp$. Thus, the assumption of Lorentz type absorption seems to be inadequate for Sm-films, but we

Table I Material parameters of garnet films. For detail see text.

Composition		$(YEuYbCa)_3(GeFe)_5O_{12}$		$(YSmLuCa)_3(GeFe)_5O_{12}$	
Ion-implantation		100 keV Ne^+ $2\times10^{14}cm^{-2}$	As-grown	100 keV Ne^+ $2\times10^{14}cm^{-2}$	As-grown
h	(μm)	3.04	3.53	3.64	3.51
l	(μm)	0.374	0.400	0.336	0.333
$4\pi M_s$	(Gauss)	263	263	278	286
K_u	(erg/cm^3)	11200	13400	15500	16000
$\gamma\times10^{-7}$	(1/sec·Oe)	1.77	1.67	2.19	2.04
α		0.036	0.038	0.16	0.16
Δ	(μm)	0.046	0.041	0.033	0.034
q		4.1	4.9	5.0	4.9
μ_{cal}	(cm/sec·Oe)	2260	1800	450	430
V_c	(cm/sec)	10100	8600	9600	9500
H_c	(Oe)	4.7	5.6	22	23
V_p	(cm/sec)	3100	2200	2000	2000
H_p	(Oe)	1.4	1.2	4.4	4.7

used this assumption even for Sm-films for convenience sake.

The q-factor $q\equiv K_u/2\pi M_s{}^2$ and the wall width parameter $\Delta\equiv(A/K_u)^{1/2}=l/2q$ were calculated from the measured material constants. In Table I are also listed the linear mobility $\mu_{cal}\equiv\gamma\Delta/\alpha$, the Walker critical velocity[8] $V_c\equiv2\pi M_s\gamma\Delta\{1+(1/2q)\}^{-1/2}$, the Walker critical field[8] $H_c\equiv2\pi\alpha M_s$, the peak velocity derived by Slonczewski[9] $V_p\equiv24\gamma A/hK_u{}^{1/2}$, and the corresponding drive field[9] $H_p\equiv V_p/\mu_{cal}$. It should be noted that all these values are calculated for a plane domain wall.

3. Experimental Results

3. 1. $S=0$, $L=2$ bubbles

The effects of an in-plane magnetic field H_{ip} on the translation velocity V of bubble domains with winding or revolution number $S=0$ and the number of vertical Bloch lines (VBL's) $L=2$ is shown in Figs. 1~4.

Figure 1 shows the results for the as-grown Eu-film. In Fig. 1 (A) H_{ip} is applied parallel to the direction of pulsed gradient field ∇H ($H_{ip}/\!/\nabla H$), and in Fig. 1(B) H_{ip} perpendicular to ∇H ($H_{ip}\perp\nabla H$). The drive field ∇H is defined as the magnitude of pulsed gradient field $|\nabla H|$ times bubble diameter along the direction of translation including the elliptic bubble deformation caused by H_{ip}. The slope of the respective straight lines drawn from the origin in Figs. 1~4 show the calculated bubble translation mobility $\mu_{cal}=2V/\Delta H$. As also shown in Fig. 5 separately, the bubble translation mobility $\mu_b\equiv2V/\Delta H$ derived from the relation between V and ΔH in low drive field region shown in Figs. 1(A) and 1(B) is only a fraction of the calculated value μ_{cal} when H_{ip} is not applied. As the increase of H_{ip}, however, it is noted that μ_b increases drastically. Bubble velocity V in high drive field region also increases as the increase of H_{ip}.

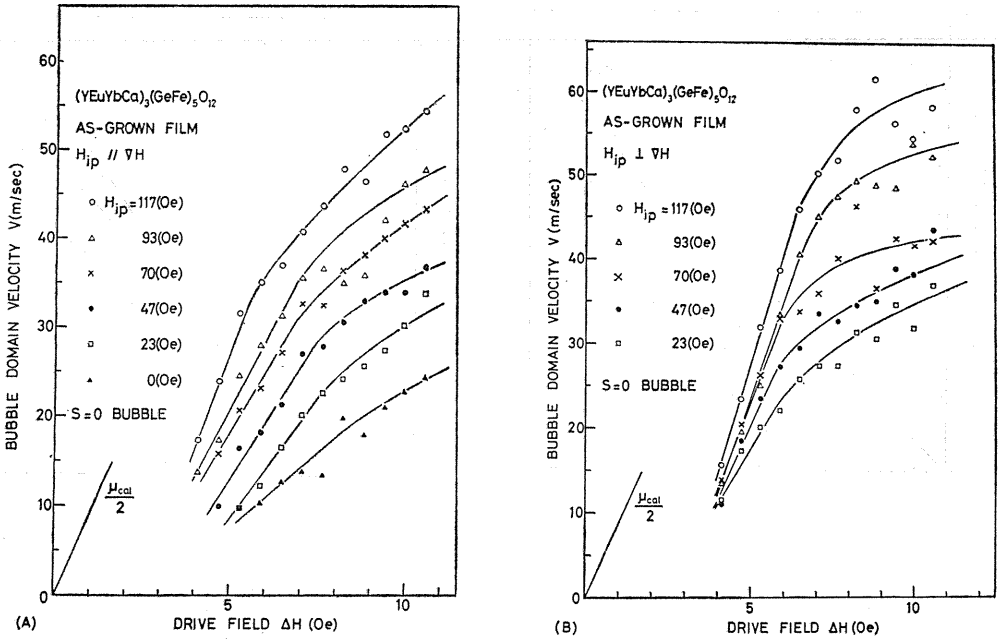

Fig. 1. Translation velocity V of $S=0$ bubble in as-grown Eu-film versus drive field ΔH with in-plane magnetic field H_{ip} as a parameter. H_{ip} is applied parallel and perpendicular to pulsed gradient field ∇H in (A) and (B), respectively.

Figure 2 shows the results for the ion-implanted Eu-film. As $S=0$ bubbles can not exist stably in ion-implanted films without H_{ip}[10], we show the result for an $S=1$, $L=0$ or unichiral $S=1$ bubble without H_{ip} for reference. The state transition from $S=0$ to $S=1/2$ becomes easier to occur with decreasing H_{ip}[11]. Therefore, we carefully set the initial bubble state to $S=0$ by the preliminary translation with sufficiently high H_{ip}. Both V and μ_b increase drastically as the increase of H_{ip} in the same manner as that in the as-grown Eu-film shown in Fig. 1. The results in the case of $H_{ip} \perp \nabla H$ are similar to those in the case of $H_{ip} // \nabla H$ shown in Fig. 2.

Figure 3 shows the results for the as-grown Sm-film having high damping constant. In contrast with the results for low damping Eu-films shown in Figs. 1 and 2, V and μ_b increase only slightly even by the application of sufficiently

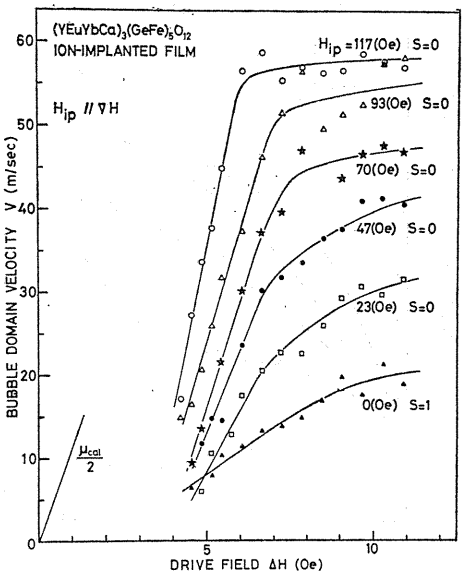

Fig. 2. Translation velocity V of $S=0$ bubble in ion-implanted Eu-film versus drive field ΔH with in-plane field H_{ip} parallel to pulsed gradient field ∇H as a parameter.

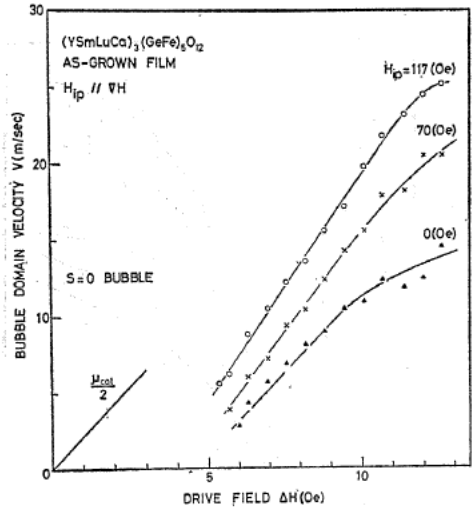

Fig. 3. Translation velocity V of $S=0$ bubble in as-grown Sm-film versus drive field ΔH with in-plane field H_{ip} parallel to pulsed gradient field ∇H as a parameter.

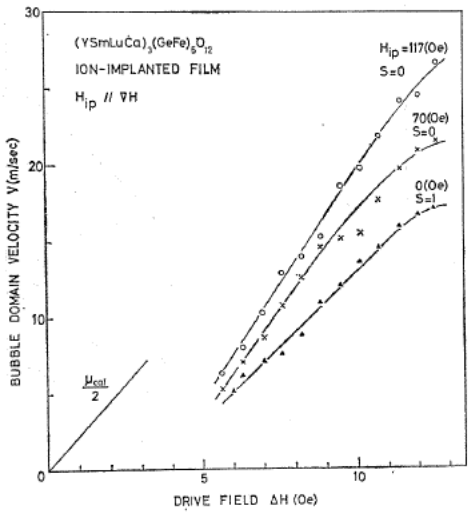

Fig. 4. Translation velocity V of $S=0$ bubble in ion-implanted Sm-film versus drive field ΔH with in-plane field H_{ip} parallel to pulsed gradient field ∇H as a parameter.

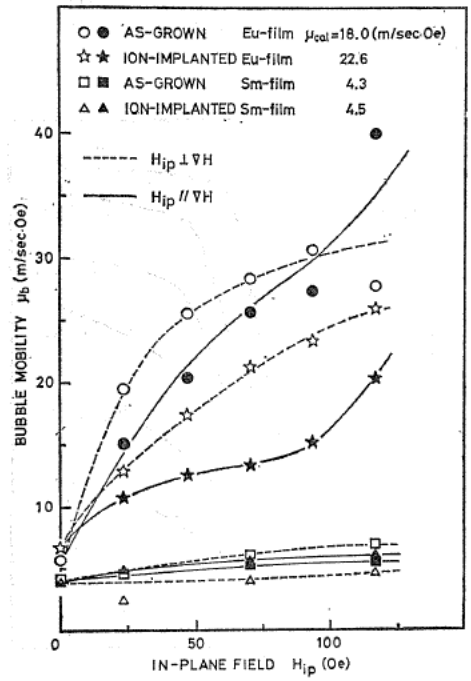

Fig. 5. Bubble translation mobility μ_b in low drive field region versus in-plane field H_{ip} derived from the results as shown in Figs. 1~4. Each curve drawn through data is only a guide to the eye.

high H_{ip}. It is noted, however, that μ_b in low drive field region without H_{ip} agrees quite well with the calculated value μ_{cal} as shown in Fig. 5. The results for the ion-implanted Sm-film shown in Fig. 4 is similar to that for the as-grown Sm-film shown in Fig. 3. The results in the case of $H_{ip} \perp \nabla H$ are again similar to those in the case of $H_{ip} /\!/ \nabla H$ shown in Figs. 3 and 4.

From these results for $S=0$ bubbles we may conclude as follows: (1) In low damping Eu-films, bubble translation velocity V and mobility μ_b increase drastically by the application of in-plane magnetic field H_{ip}. In high damping Sm-films, on the other hand, the effect of H_{ip} is very small. (2) Bubble translation mobility μ_b without H_{ip} is only a fraction of the calculated one μ_{cal} in Eu-films but agrees quite well with μ_{cal} in Sm-films. (3) In low damping Eu-films, μ_b with H_{ip} perpendicular to ∇H is generally larger than that with H_{ip} parallel to ∇H. (4) Ion-implantation for hard bubble suppression seems to affect

hardly these results.

3. 2. *S*=1, *L*=0 or *unichiral bubble*

The dependence of V of unichiral $S=1$ bubbles or $S=1$ bubbles having no vertical Bloch lines in the ion-implanted Eu-film on H_{ip} is shown in Fig. 6 where ΔH is kept constant with a value of 6.3 Oe. The maximum H_{ip} applicable to $S=1$ bubbles was limited to about 130 Oe by the occurence of the state transition from $S=1$ (skew angle χ is about 30 degrees in this sample) to $S=0$ ($\chi=0$) because the sample is ionimplanted[11]. With increasing H_{ip}, V increases slightly for H_{ip} lower than about 50 Oe but saturates very soon and remains almost constant independent of H_{ip}. It is noted that the effect of H_{ip} on V of unichiral $S=1$ bubbles is quite different from that of $S=0$ bubbles shown in Figs. 1 and 2.

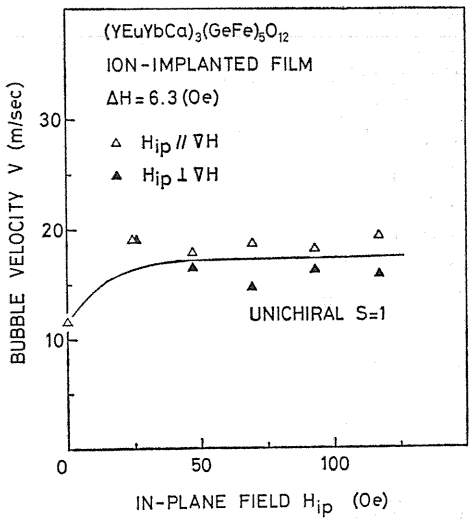

Fig. 6. Translation velocity V of unichiral $S=1$ bubble at a constant drive field $\Delta H=6.3$ Oe in ion-implanted Eu-film versus in-plane magnetic field H_{ip}.

3. 3. *S*=1, *L*=2 or *σ bubble*

σ bubble, which has been found to be propelled by gradientless bias field pulses under the application of an in-plane magnetic field by Argyle *et al.*[7], is very interesting for the present investigation because it has almost the same wall configuration as $S=0$, $L=2$ bubbles. The wall configuration of σ bubble used in the present experiment is shown in Fig. 7(C)[7] and corresponds to that of our σ_s bubble in Refs. 12 an 13. As seen from the comparison with that of $S=0$, $L=2$ bubble shown in Fig. 7(A), the

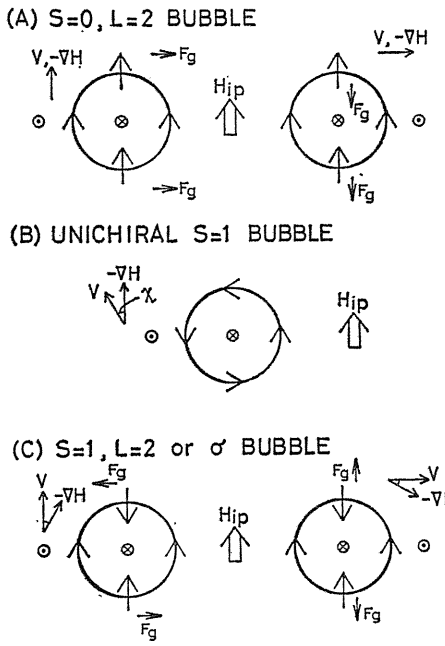

Fig. 7. Schematic representation of wall configurations of (A) the winding number $S=0$, the number of vertical Bloch lines $L=2$, (B) $S=1$, $L=0$ or unichiral $S=1$, and (C) $S=1$, $L=2$ or σ bubble, respectively. Also shown the interrelation among the directions of in-plane magnetic field H_{ip}, pulsed gradient field ∇H, bubble translation velocity V, and gyromagnetic force F_g.

wall configuration of σ bubble is the same as that of $S=0$, $L=2$ bubble except the polarity of one of the two VBL's.

Figure 8 shows the dependence of V of σ bubble in the as-grown Eu-film on H_{ip} where drive field ΔH is again kept constant with a value of 5.6 Oe. Taking account of the skew angle of $S=1$ σ bubble (about 30 degrees in this sample), H_{ip} is applied parallel or perpendicular to the direction of V. In-plane magnetic field larger than 100 Oe was applied in order to avoid the accidental bubble state change during translation. As seen in Fig. 8, V of σ bubbles is not so high even when sufficiently high H_{ip} is applied. It is noted that the dependence of V on H_{ip} for $S=1$ σ bubbles shown in Fig. 8 is quite similar to that of unichiral $S=1$ bubbles shown in Fig. 6. It is also noted that V of σ bubbles in the case of $H_{ip}\perp V$ is larger than that in the case of $H_{ip}/\!/V$.

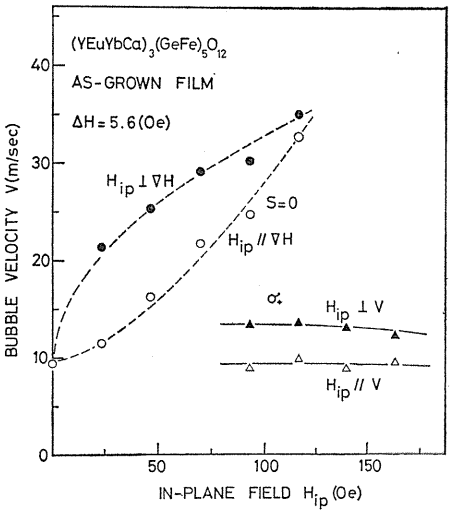

Fig. 8. Bubble translation velocity V of σ bubble in as-grown Eu-film versus in-plane magnetic field H_{ip}. Note that H_{ip} is applied parallel or perpendicular to V. Also shown that of $S=0$ bubble for comparison

4. Consideration

As for the effect of an in-plane field H_{ip} on the bubble translation velocity V, several important works have been reported so far. Bullock first investigated the effect of H_{ip} on V, and found that V increases with increasing H_{ip} and that V for H_{ip} perpendicular to gradient drive field ∇H is larger than that for H_{ip} parallel to ∇H.[4] He attributed this difference to the fact that higher mobility Bloch walls are perpendicular to V when $H_{ip}\perp\nabla H$ while lower mobility Néel walls are perpendicular to V for $H_{ip}/\!/\nabla H$. However, he did not argue at all how V is increased by the application of H_{ip}. Hsu *et al.* measured V of both an $S=0$ and an $S=1$ bubble in the presence of H_{ip}.[14] They found that V of both states increases with increasing H_{ip}, but the increase of an $S=1$ bubble is much less than that of an $S=0$ bubble. Their results are in accordance with the results shown in the previous section. Later, De Luca *et al.* studied the effect of H_{ip} on V of $S=0$ bubbles using high-speed photography.[15] In their samples were included EuGa and SmCaGe garnet films, the compositions of which are similar to those used in the present study. They measured both the bubble displacement at the end of the gradient pulse (X_T) and the final position of the bubble (X_∞) as a function of drive field ΔH at values of H_{ip} perpendicular to V. It should be noted that the "real" average velocity is X_T/T where T is the pulse width, while X_∞/T, the one shown in the last section, is the "apparent" velocity. In a EuGa sample, X_T smoothly saturates but the overshoot, the difference between X_∞ and X_T, increases with increasing ΔH at $H_{ip}=0$. Both X_T and X_∞ at a given value of ΔH increase with increasing H_{ip}. The

apparent velocity at $\Delta H \simeq 10$ Oe increases from ~ 20 m/sec at $H_{ip}=0$ to ~ 35 m/sec at $H_{ip}=100$ Oe, agreeing reasonably with the present results shown in Figs. 1 and 2. Thus, we should keep the possibility of an overshoot in mind when we interpret the data on Eu-CaGe films. Their results on a SmCaGe sample are qualitatively similar to that in a EuGa sample, but both X_T and X_∞ increase more drastically with increasing H_{ip}, X_∞/T reaching ~ 100 m/sec at $\Delta H \simeq 10$ Oe with $H_{ip}=125$ Oe. These results are contrary to the present results. This discrepancy may be attributed to the smaller damping constant of their sample, $\alpha=0.08$, compared with $\alpha=0.16$ of ours. We should rather refer to the data on the sample No. 6, a SmGa sample with $\alpha=0.2$, in their earlier work, though the effect of H_{ip} had not been examined yet.[16] In this high damping sample, X_∞ increases almost linearly with increasing drive field while X_T saturates in the high drive field region. The bubble mobility at $H_{ip}=0$ is about 3 m/secOe, agreeing quite well with the present results shown in Fig. 5. Considering further that the threshold value of ΔH below which an overshoot is not observed increases with increasing H_{ip},[15] we may consider the linear part of V versus ΔH curve in our high damping SmCaGe films to reflect the true wall mobility. Based on these and other relevant works, we consider the following three possible effects of H_{ip} on V in order to interpret the experimental results shown in 3; (1) the elliptic deformation of bubble domains, (2) the increase of domain wall velocity as revealed for infinite domain walls theoretically in Ref. 3, and (3) the suppression or enhancement of the horizontal Bloch line nucleation and the resultant overshoot during high speed domain wall motion.

4. 1. Elliptic deformation of bubble domains

Since it is difficult to measure the major diameter a and the minor diameter b of an elliptic bubble directly on the TV monitor screen with the total magnification $\sim 1400\times$, we employed the method described by Beaulieu and Calhoun.[17] When an elliptic $S=0$ bubble is translated to the direction making an angle of 45 degrees with respect to H_{ip}, the deflection angle χ_ε caused by an elliptic deformation is given by eq. (7) of Ref. 17. Substituting $\chi_0=0$ and $\phi=45°$ into this equation, the following relation is obtained.

$$\chi_\varepsilon = 3\varepsilon/4, \tag{1}$$

where $\varepsilon \equiv (a-b)/b$ is the relative bubble elongation. In the samples used in the present experiment, the deflection angle χ_ε was at most 7 degrees under the maximum H_{ip} of 160 Oe. Therefore, the maximum bubble elongation ε_{max} is estimated from eq. (1) to be at most 0.16. For simplicity, let us assume that the bubble wall is normal Bloch wall everywhere around the bubble domain and that the bubble domain is translated to the same direction as that of pulsed gradient field. Then, bubble mobility translated to the direction making an angle ϕ_0 with respect to H_{ip} is given by eq. (17) of Ref. 18 by substituting $\kappa=0$ as follows.

$$\mu_b(\phi_0) = \mu_{cal} \cdot \frac{1-(\Delta r/r_0)\cos 2\phi_0}{1-(3\Delta r/2r_0)\cos 2\phi_0}, \tag{2}$$

where $\Delta r \equiv (a-b)/2$, $r_0 \equiv (a+b)/2$ and thus $\Delta r/r_0 = (a-b)/(a+b) = \varepsilon/(2+\varepsilon)$. Note that μ_b is defined as $V/\Delta H$ in Ref. 18. Substituting the maximum bubble elongation $\varepsilon_{max}=0.16$ into eq. (2), $\mu_b(\phi_0=0°)=\mu_b(H_{ip}/\!/\nabla H)=1.04\cdot\mu_{cal}$ and $\mu_b(\phi_0=90°)=\mu_b(H_{ip}\perp\nabla H)=0.97\cdot\mu_{cal}$. Therefore, the effect of the elliptic deformation on the

bubble translation velocity and mobility is too small to explain the experimental results and presumably within experimental errors. It is also noted that the inequality $\mu_b(H_{ip}/\!/\nabla H)>\mu_b(H_{ip}\perp\Delta H)$ is opposite to the experimental results on $S=0$ bubbles in low damping Eu-films shown in Fig. 5.

4. 2. Effect of H_{ip} on domain wall velocity

Now we consider the increase of domain wall velocity caused by H_{ip}. We had previously shown the effect of H_{ip} on the velocity of an ideal one-dimensional plane domain wall by means of the direct numerical integration of the equation of motion[3]. The wall mobility μ_w normalized to that without H_{ip} or μ_{cal} is approximately given by eq. (20′) of Ref. 3 as,

$$\mu_w \equiv \frac{\mu_w}{\mu_{cal}} = 1 + \frac{2\alpha h_{x,y}}{\pi q}, \tag{3}$$

where $h_{x,y}\equiv H_{x,y}/2\pi\alpha M_s$, that is, an in-plane magnetic field applied either in the wall plane (H_x) or normal to the wall plane (H_y) normalized to the Walker critical field $H_c\equiv 2\pi\alpha M_s$. Substituting H_c and q of each sample listed in Table I and the maximum in-plane magnetic field in Fig. 5 or 117 Oe into eq. (3), the normalized wall mobility $\tilde{\mu}_w$ is estimated to be 1. 14, 1. 10, 1. 12 and 1. 11 for the ion-implanted Eu-film, the as-grown Eu-film, the ion-implanted Sm-film, and the as-grown Sm-film, respectively. The values for Sm-films show the resonable agreement with the experimental results shown in Fig. 5. Moreover, the bubble translation mobility without H_{ip} also agrees quite well with the calculated one μ_{cal}. Therefore, in high damping Sm-films the increase of the bubble translation mobility with increasing in-plane magnetic field might be explained by the increase of the domain wall velocity as described by eq. (3) for a plane domain wall.

Though it is not expressed in the approximate relation eq. (3), the fact that μ_w with H_x is larger than that with the same value of H_y as H_x is shown in the direct numerical calculation in Ref. 3. The experimental results that μ_b of $S=0$ bubbles and also V of σ bubble with H_{ip} perpendicular to V are larger than those with H_{ip} parallel to V agree qualitatively with the calculated results shown in Ref. 3, if we assume that the bubble wall portion perpendicular to V determines the value of V mainly. The similar results have been found by Bullock though he ascribed the difference between μ_b with H_{ip} perpendicular to V and that with H_{ip} parallel to V to the difference between linear Bloch wall mobility μ_B (μ_{cal} in this paper) and linear Néel wall mobility μ_N, that is, $\mu_B/\mu_N=\{1+(1/q)\}^{1/2}$ [4].

In low damping Eu-films, however, we should take account of the effect of the horizontal Bloch line nucleation because μ_b without H_{ip} is only a fraction of the calculated one μ_{cal} and the threshold drive field at which the dynamic anomaly of wall configuration may occur in a plane domain wall (H_p) is rather low as listed in Table I.

4. 3. Effect of H_{ip} on horizontal Bloch line nucleation

When H_{ip} is applied to plane domain walls, the threshold velocity V_s at which the wall structure may change due to the nucleation of horizontal Bloch lines is given by[7]

$$V_s = V_p \pm (\pi/2)\cdot\gamma\Delta H_{ip}, \tag{4}$$

where V_p is the threshold velocity without H_{ip} as listed in Table I. The plus (+) and minus (−) sign refer to the cases of wall magnetizations parallel and perpendicular to H_{ip}, respectively.

According to Bloch curve windup theory proposed by Malozemoff and Slonczewski[19], the apparent bubble translation velocity V including ballistic overshoot is given by

$$V=\frac{\mu_{cal}\Delta H}{2}\cdot\frac{V_{sat}}{V_{sat}+\mu_{cal}(\Delta H_c/2)}, \tag{5}$$

where V_{sat} is the saturation velocity or the "*true*" translation velocity of the bubble when pulsed drive field ΔH is applied, and ΔH_c is the bubble translation coercivity. In Eu-films used in the present experiments $\mu_{cal}\sim$2000 cm/sec·Oe and $\Delta H_c\sim$3 Oe; therefore, $\mu_{cal}(\Delta H_c/2)\sim$3000 cm/sec which is the same order as V_p. The accurate value of V_{sat} is unknown in the present experiments but may be estimated to be the same order as V_s. In the derivation of eq. (5) it is postulated that all the Bloch curves wound up during the application of ΔH are completely unwound to cause ballistic overshoot. In as-grown films, however, the punch-through of Bloch curves may occur. For this case, Malozemoff and De Luca has proposed an alternative model or elliptic distortion mechanism[20]. In the as-grown Eu-film used in the present experiment, however, the punch-through of Bloch curves does not occur until ΔH is increased up to ~10 Oe in the case of $S=0$ bubbles without H_{ip} as shown in Fig. 11 of Ref. 13. Therefore, we may use eq. (5) even for the results on the as-grown Eu-film in the later discussion.

The application of H_{ip} to an $S=0$, $L=2$ bubble may raise the threshold velocity V_s and thus the apparent velocity V according to eq. (5), considering the magnetostatic interaction between H_{ip} and the wall magnetization as shown in Fig. 7(A). In addition to the magnetostatic interaction, we must also take the gyromagnetic-force F_g exerted on vertical Bloch lines during bubble translation[21,22] into account, especially in the case of $H_{ip}\perp\nabla H$ (or $H_{ip}\perp V$ for an $S=0$ bubble) as pointed out by Malozemoff[23]. However, the effect of gyromagnetic force F_g may be small when the bubble translation velocity is relatively low and H_{ip} is sufficiently high. That is the case in which we are now mainly interested.

In a unichiral $S=1$ bubble, on the other hand, there exists the region where the direction of wall magnetizations is opposite to that of H_{ip}, to whichever direction H_{ip} is applied. In this case the threshold velocity V_s and thus the apparent velocity V might decrease with increasing H_{ip}. Since the result shown in Fig. 6 is taken for a unichiral $S=1$ bubble in the ion-implanted film, the bubble state may change to 1−H bubble state during translation under high H_{ip} as described by Beaulieu *et al.*[11] In any case V will be less than that expected when no dynamic anomaly occurs.

The above idea that the suppression of the horizontal Bloch line nucleation by the application of H_{ip} may lead to the increase of bubble translation velocity V, seems to explain satisfactorily why the effect of H_{ip} on V for $S=0$, $L=2$ bubbles differs from that for unichiral $S=1$ bubbles. However, the result obtained for $S=1$, $L=2$ or σ bubble makes the situation troublesome. Considering the magnetostatic interaction between H_{ip} and the wall magnetization and also considering the directions of the gyromagnetic forces shown in Fig. 7(C), σ bubble with H_{ip} applied perpendicular to V has the most favorable wall configuration. Therefore, the largest velocity increase by the application of H_{ip} might be expected for σ bubble

according to the horizontal Bloch line model. However, the translation velocity of σ bubble hardly increases with increasing H_{ip} as shown in Fig. 8.

The disagreement of the calculated domain wall velocity with that obtained experimentally, analogous to that of μ_b in low damping Eu-films shown in Fig. 5, had previously found in the case of the radial wall motion of an isolated bubble and discussed in detail by Vella-Coleiro[24]. He had concluded that current models such as the Walker model, the horizontal Bloch line model, and the spin-wave model, were inadequate to interpret the experimental data and new theories would be required.

Thus, we should also wait for the appearance of new theories in order to interpret the effect of an in-plane magnetic field on bubble domain dynamics in low damping garnet films satisfactorily.

5. Conclusion

The effect of an in-plane magnetic field H_{ip} on bubble translation velocity V and mobility μ_b was investigated by the usual bubble translation method.

In low damping Eu-films, V of $S=0$ bubbles having two vertical Bloch lines increases drastically as the increase of H_{ip}. Almost the same velocity increase is found both in the as-grown and the ion-implanted Eu-films. For $S=1$ bubbles, however, any appreciable increase of V due to H_{ip} is not found either for unichiral $S=1$ bubble or for $S=1$ σ bubble. When H_{ip} is not applied, the bubble translation mobility in low drive field region μ_b is only a fraction of the calculated one μ_{cal} both for $S=0$ and for unichiral $S=1$ bubbles.

In high damping Sm-films, on the othr hand, such a drastic increase of the $S=0$ bubble translation velocity as seen in Eu-films is not found. In this case μ_b without H_{ip} agrees quite well with μ_{cal}.

In order to interpret these experimental results were considered three kinds of effects caused by the application of H_{ip}; the elliptic deformation of bubble domains, the increase of the plane domain wall velocity, and the suppression or enhancement of the horizontal Bloch line nucleation.

The effect of the elliptic deformation of bubble domains seems to be too small to explain any experimental results. The increase of the domain wall velocity by H_{ip} as shown theoretically for an ideal one-dimensional plane wall seems to explain the experimental results obtained in high damping Sm-films rather well. The most drastic velocity increase is found for $S=0$ bubbles in low damping films. This fact suggests that the suppression or enhancement of the horizontal Bloch lines nucleation caused by the magnetostatic interaction between H_{ip} and the wall magnetization might play an important role in this case. However, the experimental results on σ bubble, which has the almost same wall configuration as that of $S=0$ bubble, seems to be opposite to the horizontal Bloch line model.

Thus, in order to explain the effect of H_{ip} on V and μ_b in low damping films satisfactorily, new theories on the domain wall dynamics seem to be required as well as further experimental investigations.

Acknowledgements

The authors would like to express our sincere thanks to Fujitsu Laboratories Ltd. for the garnet films and conductor patterns used in the experiment. We are also grateful to Mr. Orihara of Fujitsu Laboratories Ltd. and Dr. S. Tsunashima of our colleagues for their helpful discussions and encouragements.

This work was supported by the Grant-in-Aid for Scientific Research from the Ministry of Education, Science and Culture of Japan.

References

1) R. J. Rijnierse and F. H. de Leeuw: AIP Conf. Proc., No. 18 (1973) 199.
2) F. H. de Leeuw: IEEE Trans. Magn., **MAG-9** (1973) 614.
3) T. Fujii, T. Shinoda, S. Shiomi and S. Uchiyama: Jpn. J. Appl. Phys., **17** (1978) 1997.
4) D. C. Bullock: AIP Conf. Proc., No. 18 (1973) 232.
5) G. P. Vella-Coleiro and W. J. Tabor: Appl. Phys. Lett., **21** (1972) 7.
6) J. C. Slonczewski, A. P. Malozemoff and O. Voegeli: AIP Conf. Proc., No. 10 (1972) 458.
7) B. E. Argyle, S. Maekawa, P. D. Dekker and J. C. Slonczewski: AIP Conf. Proc., No. 34 (1976) 131.
8) L. R. Walker: cited by J. F. Dillon, Jr. in "*Magnetism*" edited by G. T. Rado and H. Suhl, Vol. 3, p. 450 (Academic Press, New York, 1963).
9) J. C. Slonczewski: J. Appl. Phys., **44** (1973) 1759.
10) T. Hsu: AIP Conf. Proc., No. 24 (1974) 624.
11) T. J. Beaulieu, B. R. Brown, B. A. Calhoun, T. Hsu and A. P. Malozemoff: AIP Conf. Proc., No. 34 (1976) 138.
12) S. Iwata, S. Shiomi, S. Uchiyama and T. Fujii: Jpn. J. Appl. Phys., **17** (1978) 1681.
13) S. Iwata, S. Shiomi, S. Uchiyama and T. Fujii: J. Appl. Phys., **50** (1979) 2195.
14) T. Hsu, B. R. Brown and M. D. Montgomery: AIP Conf. Proc., No. 29 (1975) 67.
15) J. C. De Luca and A. P. Malozemoff: AIP Conf. Proc., No. 34 (1976) 151.
16) A. P. Malozemoff, J. C. Slonczewski and J. C. De Luca: AIP Conf. Proc., No. 29 (1975) 58.
17) T. J. Beaulieu and B. A. Calhoun: Appl. Phys. Lett., **28** (1976) 290.
18) S. Shiomi, T. Fujii and S. Uchiyama: Jpn. J. Appl. Phys., **14** (1975) 1911.
19) A. P. Malozemoff and J. C. Slonczewski: IEEE Trans. Magn., **MAG-11** (1975) 1091.
20) A. P. Malozemoff and J. C. De Luca: J. Appl. Phys., **48** (1977) 4672.
21) A. A. Thiele: J. Appl. Phys., **45** (1974) 377.
22) J. C. Slonczewski: J. Appl. Phys., **45** (1974) 2705.
23) A. P. Malozemoff: J. Appl. Phys., **48** (1977) 795.
24) G. P. Vella-Coleiro: IEEE Trans. Magn., **MAG-13** (1977) 1163.